International Geology Review, Vol. 43, 2001, p. XXX–XXX.

Carbon and Oxygen Isotope Compositions of Some Upper Cretaceous–Paleocene Sequences in Argentina and Chile

A. N. SIAL,[1] V. P. FERREIRA,

Department of Geology, NEG-LABISE, UFPE, P.O. Box 7852, Recife, PE, Brazil, 50732-970

A. J. TOSELLI,

INSUGEO, National University of Tucuman, S.M. Tucuman, Argentina 4000

M. A. PARADA,

Department of Geology, University of Chile, P.O. Box 13518, Santiago, Chile

F. G. ACENOLAZA,

INSUGEO, National University of Tucuman, S.M. Tucuman, Argentina 4000

M. M. PIMENTEL,

Geosciences Institute, University of Brasilia, Brasilia, D.F., Brazil 70.910-970

AND R. N. ALONSO

Department of Geology, National University of Salta, P.O. Box 362, Salta, Argentina, 4400

Abstract

The Cretaceous–Paleocene (K–T) transition has been recorded in sedimentary carbonate rocks in northwestern Argentina and southern Chile. In the Yacoraite Basin, Argentina, this transition has been preserved in a 2 m thick marly layer, at the base of the Tunal Formation, which overlies lacustrine/marine carbonates of the Yacoraite Formation (Cabra Corral dam). The K–T transition is also preserved at Maimara, where Tertiary sandstones overlie a 50 m thick limestone bed of the Yacoraite Formation. In the Magellan Basin, Chile, glauconitic sandstones with calcitic cement and limestone concretions of the Maastrichtian Punta Rocallosa Formation are overlain by sandstones, claystones, and limestones of the Chorillo Chico Formation. The K–T transition is preserved in the lower portion of the Chorillo Chico Formation.

Carbonates of the Yacoraite Formation display bulk-rock $\delta^{13}C$ values from +1 to +2‰ $_{PDB}$, with a negative incursion (–4‰ $_{PDB}$) at the K–T transition. $\delta^{13}C$ values in the Tunal Formation marls vary from –3 to –1‰ $_{PDB}$. At Rocallosa Point, $\delta^{13}C$ values in limestone strata, calcite cement, and limestone concretions vary from –4 to –33 ‰ $_{PDB}$, and the lowest value in the Chorillo Chico Formation apparently marks the K–T transition. The $\delta^{18}O$ fluctuations in the Yacoraite and Magellan carbonate rocks suggest a temperature drop at the K–T transition, followed by a temperature rise.

High $^{87}Sr/^{86}Sr$ ratios (0.7140–0.7156) characterize the studied profiles of the Yacoraite Formation, documenting an important ^{87}Sr-enriched source of Sr to the water from which these carbonates precipitated. At the Magellan basin, $^{87}Sr/^{86}Sr$ ratios are closer to the expected values for the global Late Cretaceous–Paleocene ocean.

Introduction

SEVERAL STUDIES HAVE FOCUSED on the Late Cretaceous-Paleocene (K–T) transition, a time of very important worldwide massive faunal extinction. Among the several hypotheses proposed, the one by Alvarez et al. (1980) advocates faunal extinction as the result of a meteoric impact, the consequence of which was the generation of a sun-blocking dust cloud, cessation of photosynthesis, and disruption of the food chain, causing prolonged ecological modification.

In many basins where the K–T transition has been investigated using C and O isotopes, important environmental changes have been detected (e.g., Magaritz, 1989; Ferreira et al., 1994). Only in few

[1]Corresponding author; e-mail: ans@npd.ufpe.br.

FIG. 1. Location of the five K–T transition sites examined in this study in Argentina and Chile. Location of the Pernambuco-Paraíba Coastal Basin is also indicated.

places in continental South America, however, has this transition been demonstrated by stable-isotope studies of carbonate rocks. C and O isotopes are important sensors for climatic changes, and such investigations should contribute to a better understanding of this transition in the Southern Hemisphere. Suitable targets for study include sedimentary carbonate rocks of the Pernambuco-Paraíba Coastal Basin, northeastern Brazil, the Yacoraite and Neuquen basins, respectively in northwestern and west-central Argentina, and the Navidad (Topocalma Point) and Magellan (Punta Arenas) basins of Chile (Fig. 1). The Late Cretaceous–Paleocene transition also has been recorded in the Antarctic Peninsula (Souza et al., 1994), based on sedimentological, biostratigraphic, and petrologic indicators, as well as O isotopes of calcite cement and organic indicators (biomarkers and vitrinite).

C and O isotope data for carbonates from the K–T transition are available for the Pernambuco-Paraiba Coastal Basin (Albertão and Kotsoukos, 1994; Albertão et al., 1994; Ferreira et al., 1994). Albertão and Kotsoukos (1994) described a sedimentary section at the Poty quarry, in the Pernambuco-Paraíba Coastal Basin, where a 1 cm thick clay layer between the Gramame and Maria Farinha limestones exhibits distinctive features similar to clays found at the K–T transition globally, such as mass extinction, iridium and total organic C anomalies, deviations in the patterns of C and O isotopes, and exotic elements (shocked quartz grains and microspherules). This is, perhaps, the only locality in Brazil that contains the K–T transition, according to Albertão and Kotsoukos (1994). Ferreira et al. (1996) observed a sharp decrease in $\delta^{13}C$ values from +2‰ PDB to –5.5‰ PDB in the transition from the Gramame to the Maria Farinha limestone, with a corresponding increase in $\delta^{18}O$ from –6‰ PDB to –1‰ PDB that suggests a significant temperature drop at the transition, as typically observed worldwide (e.g., Magaritz, 1989).

An important climatic change during the K–T transition was recognized by Ashrof and Stinnesbeck (1989) on the basis of the fossil record of the Gramame and Maria Farinha limestones. The climate during the deposition of the Maastrichtian Gramame limestone was tropical to subtropical and changed into subtropical to temperate during the deposition of the Paleocene Maria Farinha limestone.

Oxygen isotopes studies (Hsu and Wissert, 1980) suggest that during the Late Maastrichtian, temperatures in the South Atlantic Ocean were in the 18–25°C range, with a cooling immediately before the K–T transition. A gradual temperature decrease to values as low as 10°C during the Late Maastrichtian was observed by Huber et al. (1995) studying oxygen isotopes in planktonic foraminifera from the Deep Sea Drilling Project (DSDP) in the southern Atlantic Ocean.

In this study, we examine the behavior of C, O, and Sr isotopes and bulk chemistry (Si, Mg/Ca, Sr, Fe, and Mn) of sedimentary carbonates from the Yacoraite Formation (Maimara and Cabra Corral, northwestern Argentina), the Topocalma Formation (Topocalma Point and the village of Algarrobo), Darwin's Navidad Basin (170 km southwest of Santiago), and Magellanes Province in Chilean Patagonia to evaluate evidence of a possible K–T transition. The new isotopic data will contribute to the knowledge of the geochemistry of the global ocean during the K–T transition event.

Geological Setting

K–T transition in northwestern Argentina

The K–T transition has been preserved in the transition of the Maastrichtian Yacoraite Formation to the Paleocene Olmedo Formation (Salta Group), in northwestern Argentina. This group has an evolutionary history from Early Cretaceous to Middle Paleocene and occupies a variety of sedimentary environments with a cumulative thickness of deposits of ~5,000 m (Salfity and Marquillas, 1994). The Salta Group is subdivided into the Balbuena (older) and the Santa Barbara (younger) subgroups. The Yacoraite Formation overlies the Lecho Formation and forms a part of the Balbuena Subgroup, and is overlain by the Tunal Formation (same as the Olmedo Formation; Fig. 2) of the Santa Barbara Subgroup.

According to Palma (1984), the Yacoraite Formation exhibits high-energy water facies (terrigeneous and intraclastic carbonate rocks) and quiet-water facies (claystones, mudstones, and wackestones). Carbonates include limestones, slightly magnesian to dolomitic limestones, calcitic dolomites, and dolomites. The fossil record encompasses gastropods, ostracods, pelecypods, and reptiles, as well as wood fragments, karophytas, and stromatolites that indicate lacustrine sedimentation. Lack of stratigraphic discontinuity between the Maastrichtian Yacoraite Formation and the Paleocene Olmedo Formation, led Palma (1984) to assume that the K–T transition was preserved in the Olmedo Formation.

The deposition of the Salta Group during the Neocomian to Campanian was controlled by a rift environment, but there is no unique interpretation for the depositional environment of the Yacoraite sediments. Marquillas et al. (1999) proposed that the post-rift environment was marked by a deep Maastrichtian marine ingression that marked the termination of an arid environment and led to a carbonate system that persisted until the early Paleocene.

A lacustrine depositional environment for the Yacoraite Formation sediments was recognized by Palma (1984) on the basis of observed dinosaur tracks and plant remains. Marquillas et al. (1999) assumed that the Lower Cretaceous lacustrine depositional environment graded into a marine one during the Maastrichtian, or a fluvial environment with saline mud flats with clastic and carbonate lacustrine systems until the middle Eocene. Presence of some foraminifera and fish species in the Yacoraite Formation implies a marine influence. This is a plausible hypothesis regarding sea level rise during the Late Cretaceous, and would imply that marine faunal elements could have undergone adaptation to continental conditions (Palma, 1984). Ammonites are found in Bolivia, demonstrating the existence of an open sea up to that extension of the basin, and that, to the south, there was a connection with the Atlantic Ocean, reflecting the fact that some units contain foraminifera. Yacoraite Formation limestones in some localities in Argentina contain marine fish fossils (some were flying fish; e.g., *Gasteroclupea branisai* at Tres Cruces) and, in Bolivia, these fossils were found together with ammonites. Near the top of the Yacoraite Formation in the section at Tonco Valley (dinosaur track locality), a few meters from the contact with the Paleocene Santa

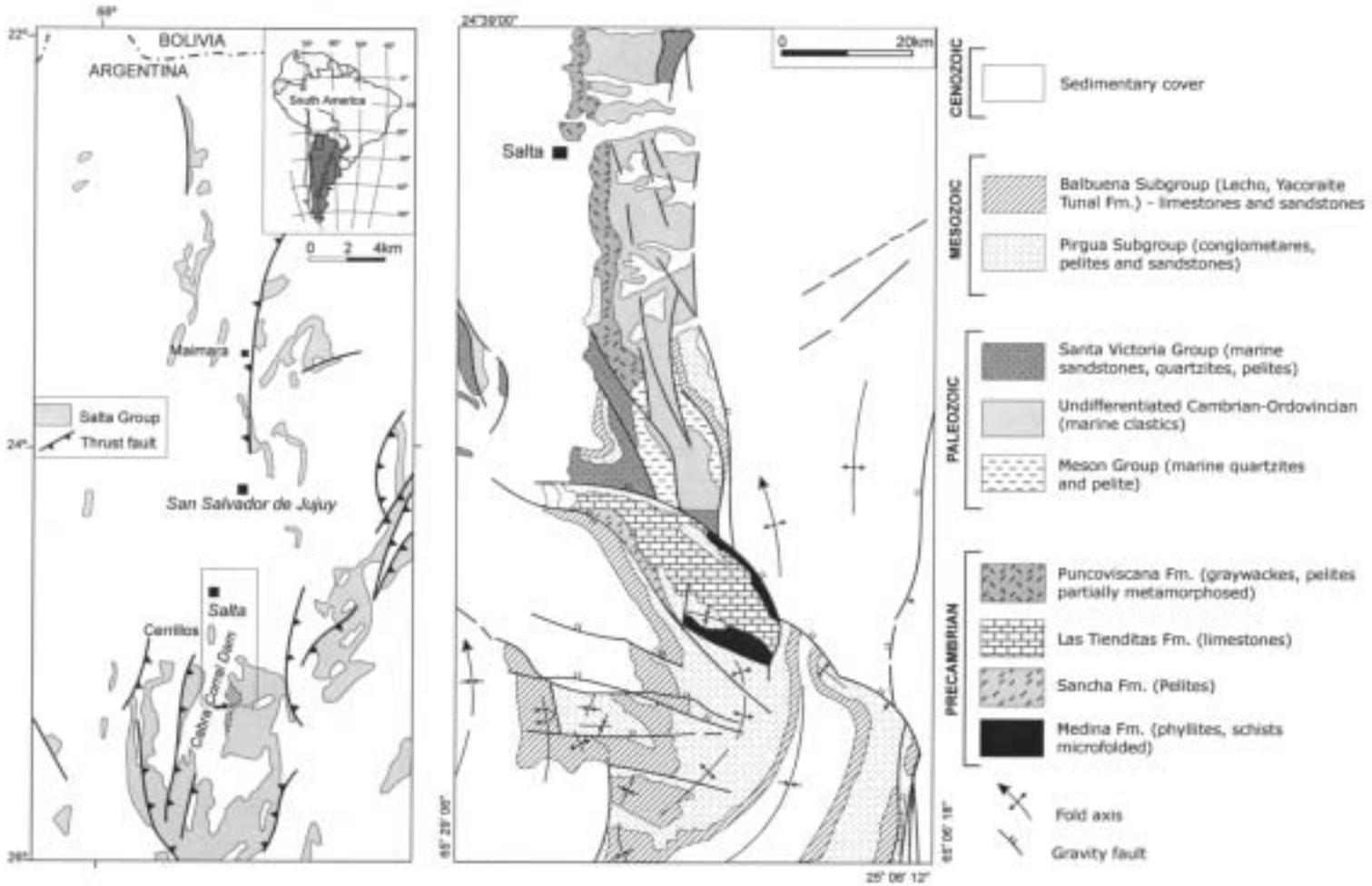

FIG. 2. A. Sites of occurrence of the Yacoraite Formation in Jujuy and Salta provinces, Argentina, including the Maimara and Cabra Corral localities. B. Geologic map of the Cabra Corral area, south of the town of Salta (after Salfity et al., 1998).

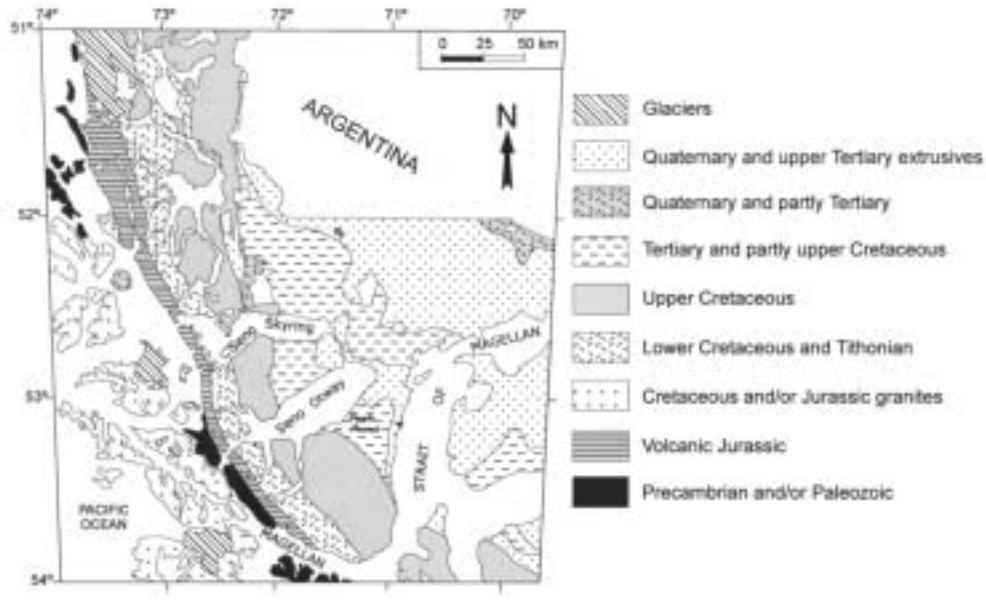

FIG. 3. Summary geologic map of southern Chile indicating areas of outcrop of upper Cretaceous and lower Paleocene sediments (modified from Ruiz, 1965).

Barbara Subgroup, there are fossils of *Coelodus toncoensis*, a typically marine fish (Benedetto and Sanchez, 1972). In Tonco Valley, in the Quebrada da Escalera section, stromatolites, ripple marks, and dinosaur tracks are abundant, although near the top of the same section, black shales and oolitic limestones with remains of fish (pycnodontiforms) are observed. Therefore, the hypothesis of lacustrine sedimentation proposed by Palma (1984) is valid only for some sectors of the basin. This basin contained, perhaps like the present-day Persian Gulf, high-evaporation lacustrine as well as open-sea environments, with a fauna adapted to great salinity variations.

Excellent exposures of the Yacoraite and Tunal formations occur at Cabra Corral dam, ~70 km south of the town of Salta, where the K–T transition seems to be complete. Yacoraite limestones are well exposed at Maimara, 70 km north of Jujuy, where they overlie red, continental sandstones of the Campanian Pirgua Formation.

The presence of mud-cracks and of a 1 cm thick gypsum layer intercalated near the top of the Yacoraite carbonate sequence at Cabra Corral dam attest to deposition at shallow depth. Fish bones and stromatolites are abundant ~10 m above the K–T transition in the Tunal Formation. There was an important environmental change in the early stages of deposition of the Tunal Formation, resulting in predominating reddish marls.

K–T transition in Chile

Charrier and Lahsen (1965, 1968, 1969) and Lahsen and Charrier (1972) made one of the first attempts to study the stratigraphy and paleontology of the K–T transition in the Punta Arenas–Strait of Magellan area (Fig. 3) of southern Chile, followed by paleoecological, sedimentological, and geochemical investigations. In the Seno Skyring area, the rocks range in age from middle Maastrichtian to early Eocene and consist of the following formations (from oldest to youngest): Fuentes, Rocallosa, Chorillo Chico, San Jorge, and Agua Fresca. The K–T transition is in the Chorillo Chico Formation, according to Charrier and Lahsen (1969).

The Rocallosa Formation, the type locality of which is on the northern coast of Riesco Island, unconformably overlies a 1220 m thick shale sequence of the late Maastrichtian Fuentes Formation (age based on foraminiferal species; Charrier and Lahsen, 1969). Along the northern coast of the Seno Skyring (Fig. 3), the contact between the Punta Rocallosa and Fuentes formations is gradational. On the southern coast of the Seno Otway (Fig. 3), the

Rocallosa Formation has lithologic characteristics that differ somewhat from the other sections.

Charrier and Lahsen (1969) divided the Rocallosa Formation, at the type locality, into four members. The lowermost 20 m thick member A is composed of glauconitic, medium- to coarse-grained, somewhat calcareous arenite, numerous concretion beds, and limestone strata. The beds do not contain terrigenous detrital material, a fact that possibly shows that they represent precipitated $CaCO_3$ from seawater. The upper Maastrichtian 60 m thick member B, at Rocallosa Point, is composed of reddish-brown sandy shale consisting of 60% carbonate matrix. It presents a sharp contact with the 100 m thick member C. This member B consists of greenish siltstone with argillaceous graywacke intercalations showing graded bedding, coarse-grained arenite lenses, and limestone-concretion layers. The lowest unit of this member is a medium-grained arenite that contains glauconite and carbonaceous remains. A layer of carbonate "concretions" of quite diverse shapes forms the top of member C, in which foraminifera point to a Late Cretaceous age. Member D consists of glauconitic, sandy siltstone with coarse glauconitic arenite intercalations, containing several beds of carbonate concretions up to 2 m in diameter. This member is more glauconitic than member C. The contact with the overlying Chorillo Chico Formation is gradational.

The type locality for the Chorillo Chico Formation is on the eastern side of Rocallosa Point, where this formation is ~275 m thick (Charrier and Lahsen, 1969) and consists of light-brown silty argillite with thin glauconitic arenite intercalations showing shaly graded beds. Coarse glauconitic arenite lenses are found at some localities and lens-shaped limestone concretions up to 6 m in diameter and 1.60 m thick are common. This formation has a more glauconitic and sandy lower member and an upper one with argillaceous graded beds and graywacke intercalations. The matrix is a reddish clay containing calcitic cement. It represents continuous K–T sedimentation.

The sedimentary sequence of Darwin's Navidad embayment overlies a Carboniferous metamorphic basement and was deposited in a NNW-striking basin, open toward the sea, located about 170km SW of Santiago at Topocalma Point on the Pacific coast. The sediments were deposited in a temperate climate and consist of three marine sequences—Cretaceous, Eocene and Miocene–Pliocene (Cecioni, 1980). The Cretaceous sediments, up to 150 m thick, have thin coquina beds at the base (bivalves), conglomerates with boulders and pebbles upward, and calcareous sandstones with large-grained quartz. Highly fossiliferous calcareous concretions are abundant. Here the K–T transition is inferred to be marked by a 0.3 m thick conglomerate layer that overlies the main coquina bed (15 m thick) and in turn is overlain by a 3m-thick sequence of non-fossiliferous sandstone with calcitic cement, bioturbated (thalassinoids), and deposited in a shallower environment.

At Algarrobo Beach, ~80 km west of Santiago, a sequence of grey, fine-grained sandstones with calcitic cement, highly fossiliferous (mainly gastropods) and with trace fossils (thalassinoids and ophiomorpha), is followed by a 0.5 m-thick conglomerate bed (pebbles, 3–5cm in diameter). The conglomerate bed is overlain for the next 3 m upsection by an apparently non-fossiliferous similar sequence containing abundant trace fossils.

Carbon, Oxygen, and Strontium Isotope Composition

Sampling and analytical methods

Roughly 200 samples were collected, at a metric scale, along traverses perpendicular to the strike of limestone layers of the Yacoraite Formation (Maimara and Cabra Corral localities), from the Topocalma Formation (Topocalma Point and Algarrobo) and from the Rocallosa and Chorillo Chico formations, not far from Punta Arenas in southern Chile. C and O isotope analyses were carried out at the Stable Isotope Laboratory (LABISE) of the Department of Geology, Federal University of Pernambuco (UFPE), Brazil. CO_2 gas was extracted from powdered carbonates in a high-vacuum line after reaction with 100% phosphoric acid at 25°C for one day (three days when dolomite was present). The CO2 released, after cryogenic cleaning, was analyzed in a double inlet, triple collector SIRA II mass spectrometer; results are reported in δ notation (‰, PDB scale). The uncertainties of the isotope measurements were 0.1‰ for carbon and 0.2 ‰ for oxygen, based on multiple analyses of an internal laboratory standard (BSC).

For determination of the Sr isotopic ratios, replicate samples were leached in 5M acetic acid and centrifuged to separate the dissolved from the insoluble fraction. Rubidium and strontium were separated from leached solutions by standard ion-exchange techniques. Strontium isotope analyses

were performed on a seven-collector Mat 262 instrument at the University of Brasilia, Brazil. Isotopic ratios have been normalized to a $^{86}Sr/^{88}Sr$ value of 0.1194.

The same samples analyzed for Sr isotopes had major elements and some trace elements analyzed by X-ray fluorescence, using fused beads and an automatic RIX-3000 (RIGAKU) unit in the Department of Geology (UFPE). Fused beads were prepared using lithium fluoride and lithium tetraborate. The whole-rock major-element analyses are listed in Table 1 and C, O, and some Sr isotope analyses and trace elements are presented.

Evaluating sample quality

Alteration, neomorphic recrystallization, diagenesis, and metamorphism can lead to post-depositional changes in the isotopic composition of sedimentary carbonates. Therefore, the use of C, O, and Sr isotopes as tools in chemostratigraphy requires precaution, and screening samples with primary isotopic values becomes imperative.

Quite a few geochemical and petrological parameters have been proposed to evaluate the degree of alteration of individual samples (see Kaufman and Knoll, 1995; Kha et al., 1999, for details). Knowledge of the behavior of Rb, Sr, Mn, and Fe helps in the selection of samples that have undergone little or no alteration. Among all the parameters used for such an evaluation, the simplest and the most effective is the Mn/Sr ratio (Kaufman and Knoll, 1995). During marine as well as meteoric diagenesis of a limestone, Mn increases and Sr decreases; therefore the Mn/Sr ratio is generally considered a good indicator of alteration (Jacobsen and Kaufman, 1999). Limestones or dolostones with Mn/Sr <10 usually retain near primary $\delta^{13}C$ abundances according to these authors. Knowledge of Mg contents helps in evaluation of the extent of dolomitization, whereas SiO_2 content reflects the presence of siliciclastics.

It is well known that oxygen isotopic compositions are sensitive indicators of diagenesis, with a decrease in $\delta^{18}O$ values characteristically resulting from isotopic exchange with meteoric or hydrothermal fluids. In most cases, crossplots of $\delta^{13}C$ and $\delta^{18}O$ commonly show no systematic variation in $\delta^{13}C$ with decreasing $\delta^{18}O$, indicating that fluid volumes sufficient to re-equilibrate O-isotopic composition were too small to have a significant effect on $\delta^{13}C$.

$\delta^{13}C$ versus $\delta^{18}O$ crossplots for each of the sampled sections from Chile (Fig. 4) show weak or no correlation. More pronounced correlation is observed for samples of the Yacoraite Formation, suggesting a secondary overprint of the oxygen isotope values. Mn/Sr ratios for the same samples, however, are significantly below 10, an indication of little secondary alteration. Samples from the Rocallosa–Chorillo Chico formations, on the contrary, exhibit Mn/Sr ratios much higher than 10, suggesting important secondary alteration. However, low values of $\delta^{13}C$ (mostly between –5 and –20‰ $_{PDB}$ with a peak value around –30‰) in carbonate cement and concretions may have been a consequence of bacterial decomposition of organic matter that may have also concentrated Mn; therefore, it is possible that the high Mn/Sr ratios are the result of processes involved in concretion formation rather than to secondary alteration.

All the C and O isotope data generated in this study were plotted on a $\delta^{18}O$ vs $\delta^{13}C$ scatter diagram (Fig. 5); this figure also displays the composition of carbonates from a variety of environments as compiled by Hudson (1977) and modified by Rollinson (1994) for comparison. Samples from the two localities in the Yacoraite Basin display a linear trend within the field for marine limestones and marbles, partially within the field for hydrothermal calcites from mid-ocean ridges, a mixing between mantle- and seawater-derived carbon. Samples from Punta Rocallosa range between the field for marine limestones/marbles and the field for early diagenetic concretions. Part of the samples from Topocalma plot within the field for marine limestones and the other half, within the field for diagenetic concretions, along almost all samples from Algarrobo Point.

Carbon and oxygen isotopes

Argentina. The two sampled sections of limestones of the Yacoraite Formation (with thin intercalations of lithographic limestones and also with stromatolites and ooids) and marls of the Tunal Formation at Maimara and Cabra Corral (Fig. 6), roughly 170 km apart, yielded similar $\delta^{13}C$ profiles. In the former, 23 samples were collected, and in the latter 24, and all were analyzed for C and O isotopes. For some of these samples, Si, Ca, Mg, Fe, Mn, Rb, and Sr also were analyzed (Table 1) in addition to $^{87}Sr/^{86}Sr$ ratios (total of 14 samples).

In both localities, $\delta^{13}C$ values of limestones of the Yacoraite Formation are essentially positive, with values up to +2‰ $_{PDB}$. However, in both sampled sections, the transition of the Yacoraite

TABLE 1. $^{87}Sr/^{86}Sr$, C and O Isotope Analyses of Representative Samples, Major- and Trace-Element Chemistry

Sample	Height,[1] (m)	$\delta^{18}O$‰, PDB	$\delta^{13}C$‰, PDB	Ca, %	Mg, %	Mg/Ca	Si, ppm	Fe, ppm	Mn, ppm	Sr, ppm	Rb, ppm	$^{87}Sr/^{86}Sr$
Yacoraite Formation, Cabra Corral Dam, Salta Province, Argentina												
YACOR 1	0.00	0.57	1.82	29.5	0.5	0.017	69799	3411	182	3120	33	0.71438
YACOR 2	6.00	1.53	2.29									
YACOR 3	5.80	2.42	2.44	19.54	4.06	0.208	108686	8443	264	2076	25	0.71569
YACOR 4	7.15	–1.24	1.68									
YACOR 5	7.00	2.52	2.21									
YACOR 6	8.40	1.55	1.14	38.52	0.32	0.008	8897	2988	136	1239	6	0.71536
YACOR 7	9.30	0.37	1.82									
YACOR 8	11.40	1.33	1.70									
YACOR 9	2.20	–1.58	1.05	38.34	0.84	0.022	5314	4926	250	1442	2	0.71430
YACOR 10	1.50	2.72	1.78									
YACOR 11	1.60	–0.25	0.93									
YACOR 12	6.50	–0.04	0.38	24.18	5.95	0.246	47044	11822	564	2388	22	0.71438
YACOR 13	6.20	–2.13	–0.19									
YACOR 14	7.25	–6.98	–1.79									
YACOR 15	0.40	–9.70	–2.93	5.33	0.76	0.143	251859	16548	745	666	111	0.71401
YACOR 16	1.00	–7.70	–4.36									
YACOR 17	2.65	–9.90	–4.06									
YACOR 18	4.00	–1.87	–2.30	28.54	0.64	0.022	66636	6447	1652	2076	30	0.71503
YACOR 19	4.60	–1.43	–2.22									
YACOR 20	6.50	–1.21	–2.29									
YACOR 21	3.40	–0.81	–1.53	30.44	1.8	0.059	38973	8647	430	4857	9	0.71565
YACOR 22	4.50	–0.79	–1.84									
YACOR 23	4.45	–0.95	–0.70									
YACOR 24	2.70	–3.27	–0.68	36.21	2.11	0.058	6776	2680	1585	1966	2	0.71474
Yacoraite Formation, Maimara, Jujuy Province, Argentina												
YAC-1	0.00	2.65	1.88									
YAC-1A	0.00	–7.99	–4.68	4.16	0.38	0.091	392970	3165	151	120	30	0.71403
YAC-1B	0.00	–12.96	–3.90	1.89	0.29	0.153	426939	2783	89	80	29	
YAC-2	2.50	4.57	2.05									
YAC-3	0.80	2.95	1.83									
YAC-4	0.65	–2.55	1.23	35.15	0.79	0.023	23001	2733	263	1217	6	

YAC-5	1.10	–2.78	1.21									
YAC-6	2.20	–1.12	1.54									
YAC-7	2.50	–0.99	1.17									
YAC-8	1.50	–1.47	1.46	37.43	0.37	0.01	20089	1731	132	826	4	0.71497
YAC-9	1.05	–2.09	1.59									0.71524
YAC-10	2.45	–1.62	1.60									
YAC-11	1.40	0.41	1.40									
YAC-12	1.30	–0.45	1.74	36.94	0.4	0.011	18379	2099	114	858	5	0.71441
YAC-13	1.20	–0.47	2.26									
YAC-14	2.20	1.08	1.59									
YAC-15	1.00	–1.24	1.11									
YAC-16	1.10	–0.26	1.37									
YAC-17	1.50	–2.20	1.36									
YAC-18	0.70	–0.62	1.31	34.03	2.77	0.081	9801	7452	237	1042	5	
YAC-19	0.20	–1.89	1.01									
YAC-20	0.70	2.96	1.78									
YAC-21	4.10	–1.56	1.42									
YAC-22	6.10	–0.34	1.62	25.37	5.04	0.199	41358	14776	286	1598	25	0.71419
YAC-23	1.50	–2.71	1.33									
					Topocalma Point, Chile							
TOPO-5	16	–1.21	–4.06	20.69	1.13	0.055	103585	32163	7251	434	12	
TOPO-7	0.90	–1.43	4.76									
TOPO-8	0.20	–1.03	–4.46	21.37	1.11	0.052	97939	32369	7152	453	11	
TOPO-15	11.95	–3.35	–9.16	17.49	0.78	0.044	143072	20308	3167	552	18	
TOPO-16	1.00	–0.60	–3.01	11.27	0.81	0.072	194269	23025	7787	614	27	
TOPO-22	9.00	0.09	–10.91	13.95	0.095	0.068	196858	22609	520	337	46	
TOPO-23	0.20	1.37	–32.34	13.97	0.81	0.058	193474	22009	524	258	41	
TOPO-24	6.00	0.66	–9.99	24.38	1.33	0.054	90567	13910	659	383	26	
TOPO-25	3.00	–0.28	–19.65									
TOPO-26	3.00	–0.01	–0.24	21.87	1.50	0.069	90450	19083	1350	419	33	
					Algarrobo Beach, Chile							
ALGA-1	0.00	–1.50	–11.02	15.32	1.43	0.094	119881	38518	5798	298	15	
ALGA-2	0.40	–1.84	–12.11									
ALGA-3	1.00	–1.37	–12.85	11.00	1.57	0.142	150646	44902	5846	203	24	
ALGA-4	0.50	–1.15	–9.82									
ALGA-6	1.00	–1.09	–11.43									
ALGA-7	0.50	–2.66	–8.13	6.55	1.78	0.271	180850	97566	2441	234	32	
ALGA-9	3.00	0.59	–14.88	5.77	1.47	0.255	210119	43100	2864	210	36	
ALGA-11	2.00	–2.14	–17.68	11.59	7,339	0.103	166403	35677	7339	277	36	

(*Table continues*)

TABLE 1. *Continued*

Sample	Height,[1] (m)	$\delta^{18}O‰$, PDB	$\delta^{13}C‰$, PDB	Ca, %	Mg, %	Mg/Ca	Si, ppm	Fe, ppm	Mn, ppm	Sr, ppm	Rb, ppm	$^{87}Sr/^{86}Sr$
						Punta Rocallosa, Patagonia, Chile						
PROCA-3	1.50	–11.14	–9.34	18.09	0.86	0.047	133698	25908	4978	176	32	0.70915
PROCA-4	1.80	–11.61	–4.46									
PROCA-5	1.50	–10.64	–6.18									
PROCA-6	2.60	–10.87	–6.89									
PROCA-7	4.60	–11.07	–5.53									
PROCA-8	3.50	–10.59	–4.99	16.04	1.01	0.063	144590	29655	5159	200	31	
PROCA-9	0.90	–11.25	–9.28									
PROCA-10	8.50	–10.88	–5.96									
PROCA-12	14.80	–11.79	–3.64	12.55	0.97	0.078	172921	27228	4893	186	52	
PROCA-14	2.70	–11.35	–4.08									
PROCA-15	1.00	–10.58	–9.41									
PROCA-17	6.80	–11.42	–3.54	12.92	1.01	0.078	160676	29809	5425	168	64	
PROCA-19	6.00	–10.63	–6.63									
PROCA-21	11.40	–11.22	–6.96									
PROCA-22	0.80	–11.50	–4.86	21.26	0.75	0.036	103079	21515	8343	166	36	
PROCA-23	0.80	–11.35	–5.86									
PROCA-25	3.00	–13.41	–15.50	5.35	1.09	0.203	251684	35955	985	281	48	
PROCA-30	17.30	–7.83	–5.50	2.63	1.05	0.401	266645	39680	597	311	44	
PROCA-31	0.60	–8.90	–5.29									
PROCA-32	2.50	–8.65	–6.95									
PROCA-35	6.00	–7.51	–5.26									
PROCA-36	1.20	–8.87	–8.72	26.73	0.51	0.019	70444	15598	6756	392	16	0.70776
PROCA-41	16.10	–10.99	–11.54									
PROCA-42	5.50			2.32	1.1	0.474	272221	40745	605	300	46	0.70733
PROCA-43	9.50	–8.30	–6.72									
PROCA-45	9.80	–7.83	–11.54									
PROCA-46	6.00	–10.34	–13.30	20.50	0.64	0.031	108391	20497	7461	256	30	
PROCA-47	0.30	–8.72	–7.41									
PROCA-49	39.00	–10.77	–12.67									
PROCA-50	9.50	–11.45	–10.36	24.07	0.60	0.025	84805	18941	6291	224	33	
PROCA-51	9.00	–10.30	–10.90									
PROCA-53	15.00	–8.11	–4.78									
PROCA-54	5.00	–8.14	–15.22	25.93	0.58	0.023	70133	15142	2644	347	14	

PROCA-55	2.50	–11.68	–7.44									
PROCA-56	30.00	–10.49	–7.81									
PROCA-57	5.20	–10.96	–8.82									
PROCA-59	8.70	–6.87	–13.05									
PROCA-60	9.80	–11.77	–8.26	18.13	0.82	0.045	126985	25795	6772	187	37	
PROCA-61	9.80	–11.70	–9.57									
PROCA-62	2.50	–12.08	–6.23									
PROCA-63	14.00	–11.90	–10.03									
PROCA-64	54.00	–10.84	–11.16									
PROCA-65	8.00	–11.65	–3.84									
PROCA-66	14.00	–11.17	–9.96									
PROCA-67	29.00	–9.40	–9.17	20.12	1.03	0.051	127148	22233	2796	545	24	
PROCA-68	2.70	–4.75	–33.17	26.89	0.81	0.049	74280	10957	1837	646	11	
PROCA-69	49.00	–11.81	–4.26	11.56	0.81	0.070	164766	27499	5859	591	45	
PROCA-70	9.30	–12.10	–8.92	14.07	0.85	0.061	160883	20188	6635	384	37	0.70667
PROCA-71	21.00	–12.48	–9.44									
PROCA-72	58.00	–11.65	–10.25									
PROCA-73	3.50	–7.03	–4.00									
PROCA-74	27.00	–13.31	–5.63	17.52	0.84	0.048	133214	22368	7863	401	49	
PROCA-75	19.00	–4.42	–19.91									
PROCA-76	10.00	–5.25	–20.23									
					Altamirano Point, Patagonia, Chile							
PALTA-10	0.00	–5.90	–22.78	26.69	1.02	0.038	72806	15907	6847	383	21	
PALTA-9	6.00	–8.09	–16.16	26.33	0.65	0.025	74238	16809	10948	184	18	
PALTA-1	12.50	–8.46	–19.07	26.01	0.75	0.029	70596	24307	12157	138	24	
PALTA-2	6.50	–8.33	–19.84									
PALTA-5	95.00	–9.02	–18.52	16.07	1.44	0.089	126614	46564	94036	224	50	
PALTA-6	4.00	–8.49	–19.32									
PALTA-7A	0.50	–8.29	–19.02									
PALTA-7	0.50	–7.15	–21.45									
PALTA-8	4.00	–8.43	–15.59									

[1]Stratigraphic position in relation to the previous sample of the section.

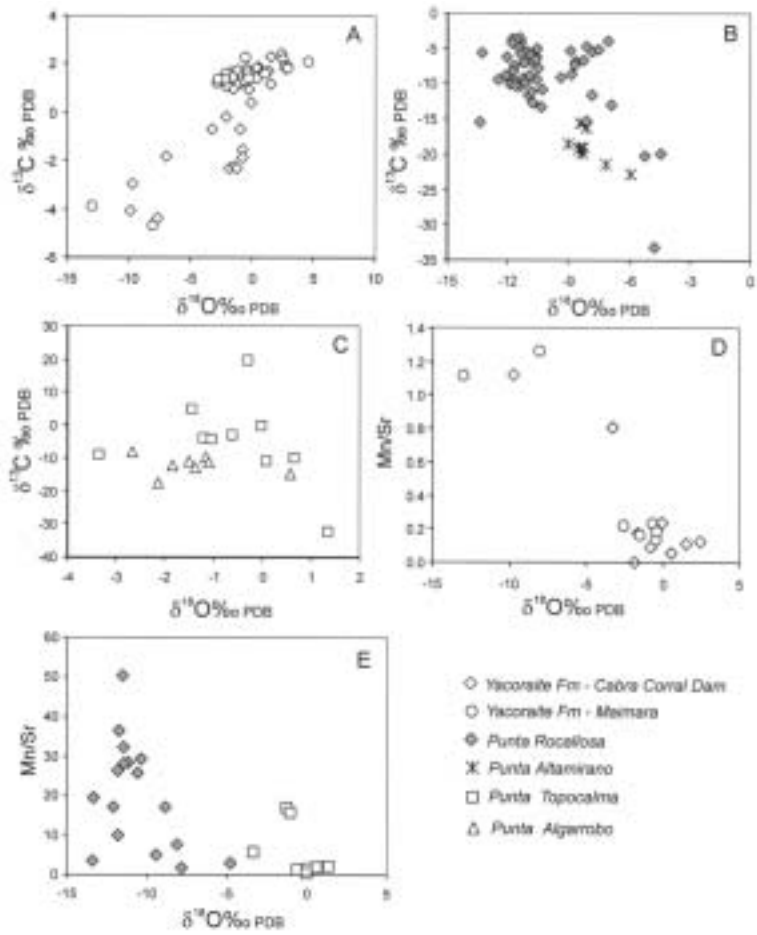

FIG. 4. $\delta^{13}C$ vs. $\delta^{18}O$(‰ $_{PDB}$) for the Yacoraite-Tunal formations in Maimara and Cabra Corral at (A), for the Punta Rocallosa–Chorillo Chico formations at (B), and Punta Topocalma and Algarrobo at (C). Mn/Sr ratios versus $\delta^{18}O$ (‰ $_{PDB}$) for the Yacoraite-Tunal formations at (D) and for the Punta Rocallosa–Chorillo Chico formations at (E).

limestones to purple-greenish marls of the Tunal Formation (Cabra Corral section) or sandstone with calcite cement (Maimara section) is marked by a strong shift of $\delta^{13}C$ to values ~–5‰$_{PDB}$, which in the Cabra Corral section is followed by a gradual increase. This isotopic behavior seems to match those of K–T transition sites studied elsewhere (e.g., Magaritz, 1989).

The two studied sections of the Yacoraite Formation display a similar behavior of oxygen isotopes, with a gradual decrease of $\delta^{18}O$ near the K–T transition. Considering these values to be primary or close to that, a temperature drop followed by substantial temperature increase right after the transition can be inferred.

Chile. The Rocallosa and the Chorillo Chico formations were sampled, at a metric scale, in two sections: (1) Rocallosa Point, along the northern margin of Riesco Island; and (2) Altamirano Bay on the opposite side. Both sections are located in the Seno Skyring area. At Rocallosa Point, 76 samples were collected, from which 54 were analyzed for C and O isotopes, whereas in Altamirano Bay, 10 samples were collected. For some of these samples, Si, Ca, Mg, Fe, Mn, Rb, and Sr also were analyzed and in 4 samples $^{87}Sr/^{86}Sr$ ratios were determined (Table 1).

In the first of these two profiles, the Rocallosa Formation is constituted by fine to medium-grained, slightly shaly, sandstones with calcite cement, limestone strata, and large spherical limestone concre-

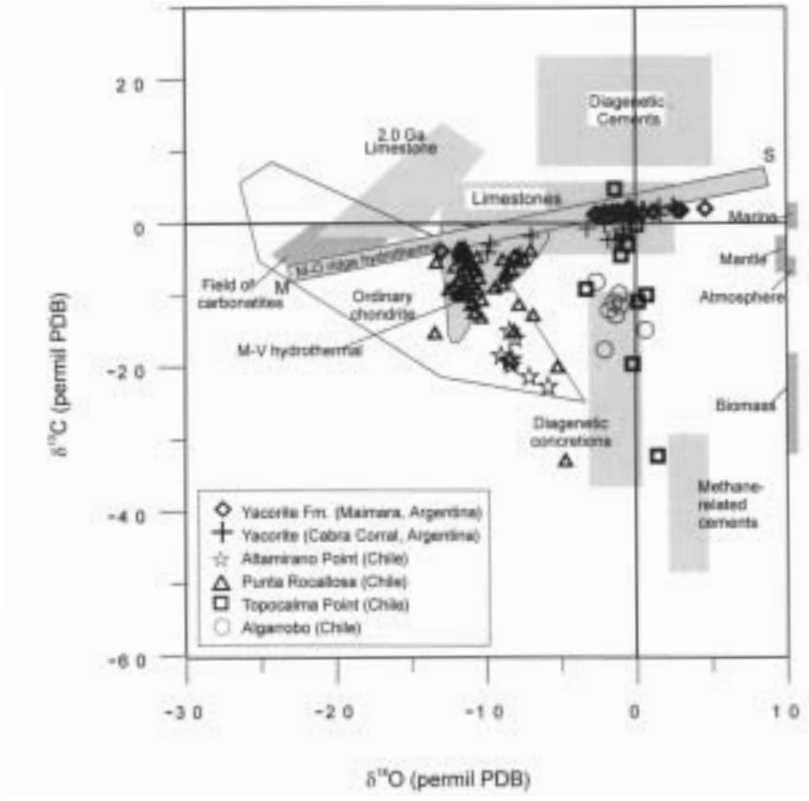

FIG. 5. Typical compositions are displayed on a $\delta^{13}C$ versus $\delta^{18}O$(‰ PDB) scatter diagram for all samples in this study. The typical composition for carbonates from a variety of environments ($\delta^{18}O$) also is plotted relative to SMOW scale. Based on Hudson (1977), modified by Rollinson (1994).

tions. The Chorillo Chico Formation in this section is represented by shaly, glauconitic siltstones, with thin limestone strata and limestone lens-shaped concretions, elongate parallel to stratification, which are more abundant than in the Rocallosa Formation. Lithologically, this formation is similar to the previous one, except for the size of the grains. Several centimeter-thick glauconitic beds were observed in what we consider to be the base of the Chorillo Chico Formation. The contact between the two units in the sampled locality is represented by a rather continuous sedimentation. The gradation between the two formations is characterized by meter-scale drag folds with almost vertical fold axes. At Punta Rocallosa, sandstones show many black, angular to rounded volcanic fragments, and small volcanic bombs, all of mapproximately the same size. There is no clear field evidence of where exactly the K–T transition (supposedly within the Chorillo Chico Formation, according to Charrier and Lahsen, 1965), was recorded along the two examined sections.

C-isotopic trends across the studied section at Rocallosa Point markedly differ from those observed at Maimara and Cabra Corral in Argentina. Analyzed samples (sandstone with calcite cement, limestone concretions, and limestone strata) exhibit negative $\delta^{13}C$ values, ranging from –3.6 down to –33‰$_{PDB}$ (Fig.7); however, most of the samples range about –10‰ $_{PDB}$, irrespective of lithological characteristics (limestone concretion or sandstone/shale with calcite cement). A significant shift to a value of –33‰ $_{PDB}$ recorded within the Chorillo Chico Formation, about 3 m above its contact with the Rocallosa Formation, has been interpreted as a possible location for the K–T transition (also foreseen by Charrier and Lahsen, 1965). The $\delta^{13}C$ values of around –10‰ $_{PDB}$ predominate in the Punta

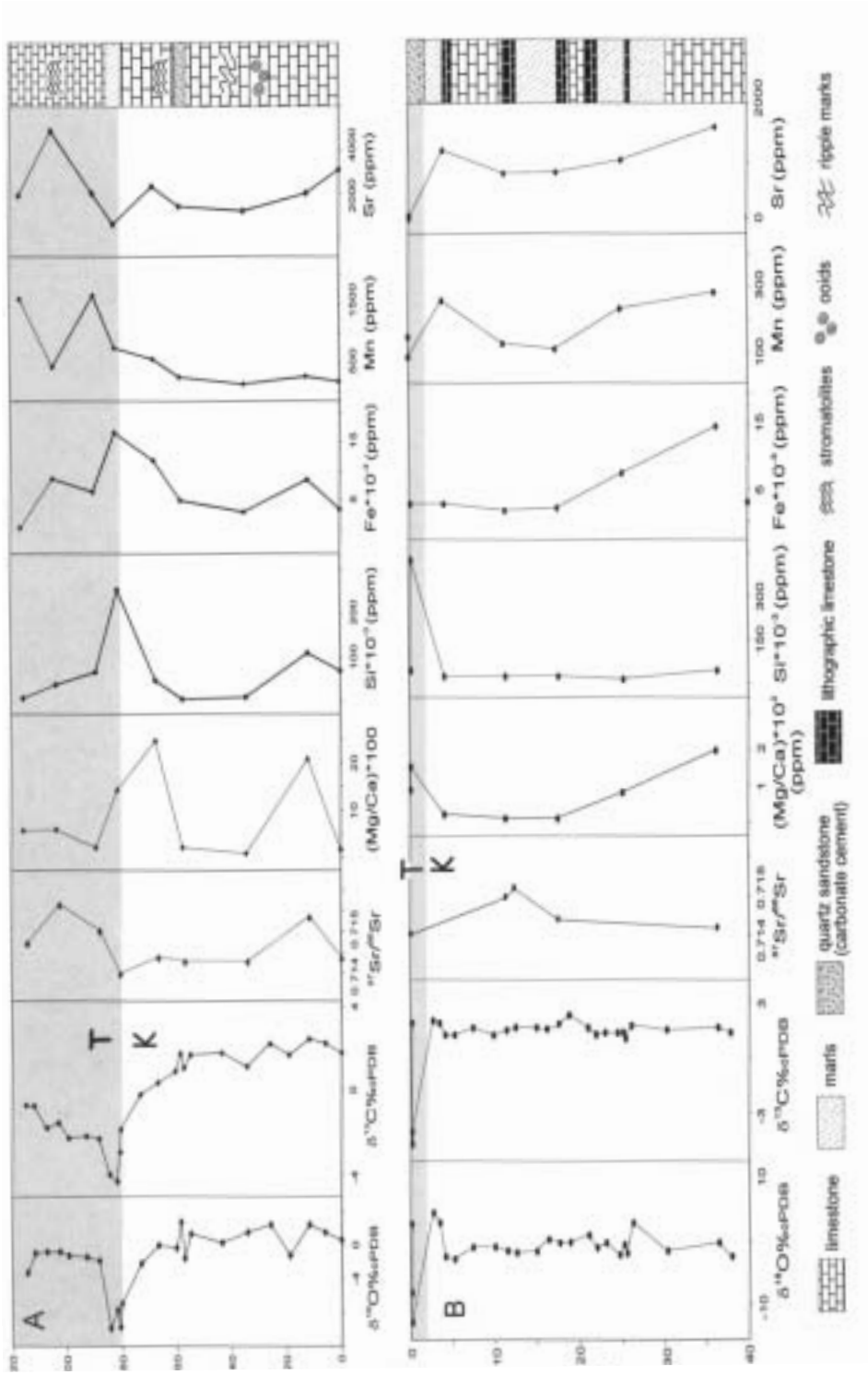

FIG. 6. Chemostratigraphy including $\delta^{13}C$, $\delta^{18}O$, and $^{87}Sr/^{86}Sr$ and some major and trace elements in carbonate rocks along the stratigraphic column of the Yacoratite Formation at Cabra Corral, Salta Province (A) and at Maimara, Jujuy Province (B), in Argentina.

Rocallosa Formation, whereas at the Chorrilo Chico Formation values are mostly between –10‰ $_{PDB}$ and –15‰ $_{PDB}$, fluctuations being gradually attenuated upsection toward values of around –5‰ $_{PDB}$. Samples from the section at the Altamirano Point (not shown), which are mostly from limestone concretions, show $\delta^{13}C$ in the –16 to –23‰ $_{PDB}$ range without any major shift to more negative values.

Marine inorganic carbon has $\delta^{13}C$ around 0‰ $_{PDB}$, and highly negative values in the present study indicate considerable organic carbon that ends up in CO_2. The CO_2 generated in the sulfate-reduction zone (a few centimeters to decimeters below sea level) can reach –15 to –25‰ $_{PDB}$ levels. Slightly deeper, in the zone of anaerobic oxidation, methane can generate CO_2 of equally or more negative values. A value of –33‰ $_{PDB,}$ as observed here, is common in shale concretions (Mozley and Burns, 1992) and suggests that most of the carbon was derived by bacterial processes.

Samples from Rocallosa and Altamirano points show much higher concentrations of Mn (Table 1) than the Yacoraite Formation in Argentina, and consequently the Mn/Sr ratios are much higher (up to 50). This behavior is probably a consequence of the bacterial activity in the limestone concretion formation. Oxidation of organic matter in this process probably led to oxidation of Fe, with Fe^{+2} being partially replaced by Mn.

Oxygen isotopes range from –5 to –13‰ $_{PDB}$, with an important shift to less negative values (–5‰ $_{PDB}$) at the point where the minimum $\delta^{13}C$ value has been recorded. The upper portion of the Chorillo Chico Formation (~ 60 m) shows a relatively consistent behavior around –11‰$_{PDB}$. The $\delta^{18}O$ profile does not exhibit any covariance with $\delta^{13}C$, which favors primary signatures. If so, the oxygen isotope behavior can be interpreted in terms of an important temperature decrease at the K–T transition, in consonance with observations elsewhere in the South Atlantic Ocean (Hsu and Wissert, 1980; Huber et al., 1995).

The C, O profiles for the sections at Topocalma Point and at Algarrobo Beach were less informative than the ones examined in Argentina and at Rocallosa Point. They do not represent continuous carbonate sections, and the limestone concretions developed during a diagenetic process around a large amount of shells; it is uncertain if the diagenesis was early or late. Ten samples from Punta Topocalma were analyzed for C and O isotopes. The $\delta^{13}C$ values are negative, with a minimum of –30‰ $_{PDB}$

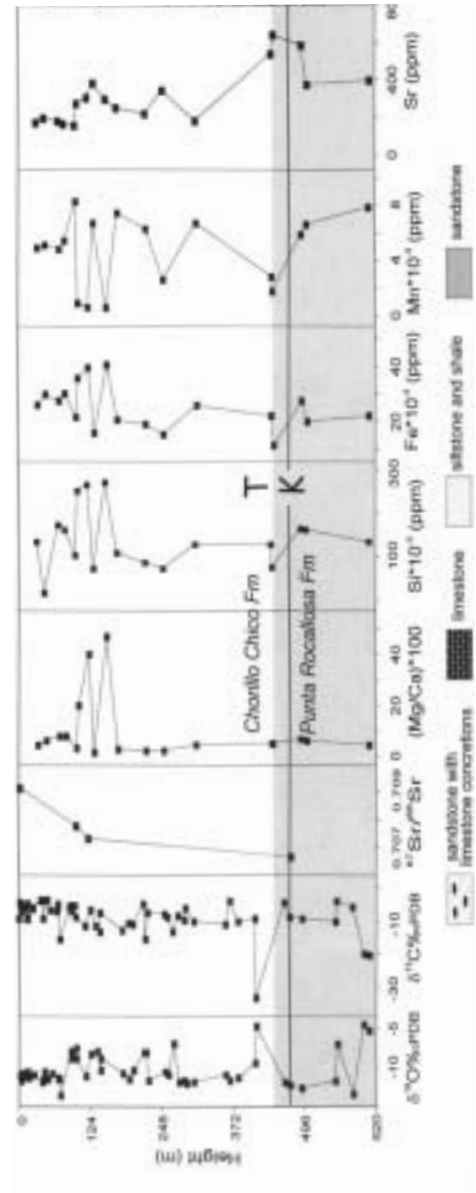

FIG. 7. Chemostratigraphy including $\delta^{13}C$, $\delta^{18}O$, $^{87}Sr/^{86}Sr$, and some major and trace elements in carbonate rocks along the stratigraphic column of the Punta Rocallosa and Chorillo Chico formations, Chilean Patagonia.

(sample collected in a coquina bed that underlies a 0.3 m thick conglomerate layer) that may correspond to the K–T transition; however, the $\delta^{13}C$ chemostratigraphic profile obtained (not shown) is of dubious interpretation, as almost all the analyzed samples are from calcareous concretions.

Some major and trace elements (Ca, Mg, Si, Sr, Rb, Mn, and Fe) were analyzed in eight samples. The Fe contents gradually decrease upsection, whereas Mn behaves the opposite way. This suggests that possibly Fe^{+2} was gradually replaced by Mn in the calcareous concretions analyzed as a consequence of bacterial activity. In three samples, the Mn/Sr ratio is greater than 10 as a result of this process. Strontium has lower concentrations in this section than in samples from the Yacoraite Formation.

C and O isotopes were analyzed in eight samples in a 10 m section (not shown). At Algarrobo Beach, $\delta^{13}C$ values range from –8 to –18‰ $_{PDB}$ (with most values around –11‰ $_{PDB}$), and become more negative in the last 3 m upsection (only two samples that correspond to non-fossiliferous sandstone/shale with abundant trace fossils were analyzed in this interval). The $\delta^{18}O$ varies from +0.6 to –2.1‰ $_{PDB}$, a range similar to that at the Topocalma section, but much higher than the range observed at Punta Rocallosa. Some major and trace elements (Si, Mg, Ca, Fe, Mn, in addition to Sr and Rb) analyzed in five of these samples, reveal higher Fe content than samples at the Topocalma profile, but with much less Sr with Mn/Sr ratios greater than 10. As in this section, we are not dealing with carbonate concretions, and consequently cannot invoke bacterial action to justify high Mn/Sr ratios. Therefore, we cannot assure that the observed isotope ratios in these analyses are primary.

Strontium isotopes

Variations of $^{87}Sr/^{86}Sr$ (r_0) ratio in seawater are primarily due to variations in continental erosion rates as well as variations in the Sr isotope composition of the input to the oceans. Changes in this isotopic ratio are usually linked to major tectonic events.

The evolution of the oceanic strontium isotopic ratio seems to be well constrained for the Phanerozoic (Godderis and François, 1995, and references therein) and particularly since the Jurassic (e.g., Denison et al., 1993; Jones et al., 1994). If the general trend is considered, higher values characterize the Late Neoproterozoic (0.709) followed by lower values during much of the Paleozoic and Mesozoic eras (0.707). A sharp increase is observed during the Cenozoic (after 40 Ma) to the present value (0.709). There is a small drop of the r_0 right after the K–T transition in the curve presented by Burke et al. (1982).

The reason for the many oscillations observed and, in particular, the Cenozoic evolution of the strontium cycle, was discussed and modeled by Godderis and François (1995). They postulated that the Cenozoic increase in the seawater $^{87}Sr/^{86}Sr$ ratio could have been associated with the uplift of the Himalayan and Andean mountains that had an impact on the Sr cycle, contributing Sr with particularly high $^{87}Sr/^{86}Sr$ ratios to oceans through the major rivers draining these areas. In addition, Basu et al. (2001), studying the groundwater flux to the oceans from the Bengal Basin in India, concluded that this type of flux can be potentially a significant source of strontium to the oceans, in some cases equal in magnitude to the dissolved strontium concentrations carried to the oceans by river waters.

Strontium isotope ratios have been analyzed in nine samples of the Yacoraite Formation from the Cabra Corral profile, and in five samples from the Maimara profile. The observed $^{87}Sr/^{86}Sr$ variation (0.71403 to 0.71565; Fig. 6; Table 1) in the Cabra Corral profile confirms that early carbonates of this formation were mostly deposited in a lacustrine environment, as documented by the paleontological record, with a probably important continental influence on the Sr isotope ratios. The samples with the lowest values of this ratio (0.714) are also those with the lowest $\delta^{13}C$ and $\delta^{18}O$, and occur in the stratigraphic level where we assume the K–T transition was possibly recorded (Fig. 6). An important chemical change is observed at about half way up this stratigraphic profile, with an increase in the Mg/Ca ratio, Si, Fe, and Mn concentrations. These changes are a proxy for important environmental changes that accompanied the K–T transition in this area, and were responsible for an increase in radiogenic ^{87}Sr. After the transition, a tendency for a decrease of Mg/Ca, Si and Fe with a slight increase in Mn and Sr is evident.

At the K–T transition in Maimara, $\delta^{13}C$ and $\delta^{18}O$ values shift to lower values (Fig. 6B) than at the section in Cabra Corral. The section at Maimara also shows less SiO_2 variation throughout the entire section than the Cabra Corral profile, with a significant increase only around the K–T transition. In both sections, the $^{87}Sr/^{86}Sr$ values (Fig. 6, Table 1) spread within the same range, with an important decrease in the last stages of deposition of the Yacoraite For-

mation. At Cabra Corral, this is followed by an increase of this ratio in the Tunal Formation.

As these K–T carbonates are located near the Andean chain, their $^{87}Sr/^{86}Sr$ values probably reflect the influence of early uplift and subsequent erosion of the chain. Groundwater flux also could have had some influence on the $^{87}Sr/^{86}Sr$ of these carbonates, because part of them were deposited in a lacustrine environment.

Strontium isotope ratios in four samples from carbonate strata at the Punta Rocallosa section (Table 1) show a peak at the proposed K–T transition, followed by an upsection decrease. A $^{87}Sr/^{86}Sr$ value of 0.70667 was determined in a sample from the Punta Rocallosa Formation at the base of the section, and progressively higher values were observed in the Chorillo Chico Formation (0.70733, 0.70776, and 0.70915). This isotope variation is within the range of variation of seawater $^{87}Sr/^{86}Sr$ around 65 Ma (Burke et al. 1982; Howarth and McArthur,1997). Si, Fe, and Mn decrease in the transition (Fig. 7), an opposite behavior of what has been observed in the two studied sections in Argentina.

Conclusions

This investigation has shown that sedimentary carbonates of the Yacoraite Basin in northwestern Argentina recorded a possible temperature drop during the K–T transition, followed by increase in the early Paleocene. This is in agreement with the cosmogenic hypothesis for the transition, where an important cooling would be expected, followed by a temperature increase in response to the greenhouse effect. These carbonates also record an important negative $\delta^{13}C$ incursion, similar to what has been observed worldwide. Strontium isotope ratios (r_0) in carbonates of the Yacoraite Formation are far too high relative to values predicted in the r_0 worldwide curve. It seems that during the stage during which carbonates were deposited in a lacustrine environment in the Yacoraite Basin, the Sr cycle was greatly influenced by an ^{87}Sr-enriched continental sources supply. Evidently carbonates deposited towards the top of the analyzed sections have also been influenced by an ^{87}Sr–enriched cycle.

Oxygen isotopes of carbonates from limestone strata in the Magellan Basin, Chile, recorded climatic behavior similar to that registered by Yacoraite Basin carbonates, also suggesting a cooling at the base of the Chorillo Chico Formation, followed by a temperature increase. This behavior is in close agreement with that reported by Ferreira et al. (1994, 1996) for the Pernambuco-Paraiba basin, in northeastern Brazil. The $\delta^{13}C$ fluctuations in the latter, however, are all positive, except for an important drop from $+2‰_{PDB}$ to $-5.5‰_{PDB}$ at the K–T transition in the Gramame/Maria Farinha formation limestones in the Pernambuco-Paraíba Coastal Basin, accompanied by an increase in $\delta^{18}O$ (from –6 to $-3‰_{PDB}$) to $-1‰_{PDB}$, corresponding to an important temperature drop at the transition. In Chilean Patagonia, however, the Punta Rocallosa and Chorillo Chico formations show more "normal" $^{87}Sr/^{86}Sr$ ratios.

Acknowledgments

This research was partially supported by the VITAE grant no.11487/B009. We express our gratitude to Vilma S. Bezerra and Gilsa M.de Santana for assistance with the C and O isotope analyses at the Stable Isotope Laboratory (LABISE) and to Isaias Barbosa for the XRF analyses in the Federal University of Pernambuco. Information concerning carbonate concretions and C isotope behavior by E. F. McBride (Austin, Texas) in an early stage of development of this study was very useful. We thank Rielva S. Nascimento and Roberta G. Brasilino for assistance in preparation of the figures, and Simone Gioia and Maria Helena B. M.de Hollanda for assistance with Sr isotope analyses at the University of Brasilia. This is the NEG-LABISE contribution No. 182.

REFERENCES

Albertão, G. A., and Koutsoukos, E. A. M., 1994, The Cretaceous–Tertiary boundary in Pernambuco, northeastern Brazil, *in* 14th International Sedimentological Congress, Recife. Field Guide to the Poty Quarry Section, p. 1–14.

Albertão, G. A., Koutsoukos, E. A. M., Regali, M. S. P., Attrep, M., Jr., and Martins, P. P., Jr., 1994, The Cretaceous–Tertiary boundary in southern low-latitude regions: Preliminary study in Pernambuco, northeastern Brazil: Terra Nova, v. 6, p. 366–375.

Alvarez, L. W., Alvarez, W., Asaro, F., and Michael, H. V., 1980, Extraterrestrial cause for the Cretaceous/Tertiary extinction: Science, v.208, p. 1095–1108.

Ashrof, A. R., and Stinnesbeck, W., 1989, Pollen und sporen and der Kreide-Tertiagreenze in Staate Pernambuco NE Bresilien: Paleont-gr. Abt. B, v. 208, nos. 1–3, p. 133–149.

Basu, A. R., Jacobsen, S. B., Poreda, R. J., Dowling, C. B., and Aggarwal, P. K., 2001, Large groundwater strontium flux to the oceans from the Bengal Basin and the marine strontium isotope record: Science, v. 293, p. 1470–1473.

Benedetto, J. L., and Sánchez, T. M., 1972. Coelodus toncoensis nov. sp. (Pisces, Holostei, Pycnodontiformes) de la Formación Yacoraite, Cretacico Superior de la Provincia de Salta: Ameghiana, v. IX, p. 59–71.

Burke, W. H., Denison, R. E., Hetherington, E. R. A, Koepnick, R. B., Nelson, H. F., and Otto, J. B., 1982, Variations of seawater $^{87}Sr/^{86}Sr$ throughout Phanerozoic time: Geology, v. 10, p. 516–519.

Cecioni, G., 1980, Darwin's Navidad Embayment, Santiago Region, Chile, as model of the southeastern Pacific Shelf: Journal of Petroleum Geology, v. 23, p. 309–321.

Charrier, R., and Lahsen, A., 1965, El limite Cretaceo-terciario entre el Seno Skyring y el Estrecho de Magallanes: Unpubl. thesis, School of Geology, Universidad de Chile, Santiago, p. 34–54.

_____, 1968, Contribution a l'étude de al limite Crétacé-Tertiaire dans la Province de Magellan, extreme sud du Chili: Revue Micropaleontologie, v. 111, p. 111–120.

_____, 1969, Stratigraphy of Late Cretaceous–Early Eocene Seno Skyring–Strait of Magellan area, Magallanes Province, Chile: American Association of Petroleum Geologists Bulletin, v.. 53, p. 568–590.

Denison, R. E., Koepnick, R. B., Fletcher, A., Dahl, D. A., and Baker, M. C., 1993, Reevaluation of Early Oligocene, Eocene, and Paleocene seawater strontium isotope ratios using outcrop samples from the U.S. Gulf Coast: Paleoceanography, v. 8, p. 101–126.

Ferreira, V. P., Sial, A. N., Chaves, N. S., and Brasilino, R. G., 1994, Stable isotopes and the K–T boundary in the Pernambuco Basin, *in* 14th International Sedimentological Congress, Recife, p. S3-4–S3-5.

Ferreira, V. P., Sial, A. N., and Menor, E. A., 1996, Carbon and oxygen isotopes in offshore and continental Mesozoic and Tertiary limestones, NE Brazil: The K–T boundary and Tertiary climatic variations: Acta Geologica Hungarica, v. 39, suppl., p. 43–46.

Godderis, Y. and François, L. M., 1995. The Cenozoic evolution of the strontium and carbon cycles: Relative importance of continental erosion and mantle exchanges: Chemical Geology, v. 126, p. 169–190.

Howarth, R. J., and McArthur, J. M., 1997. Statistics for strontium isotope stratigraphy: A robust LOWESS fit to the marine strontium isotope curve for the period 0 to 206 Ma, with look-up table for the derivation of numerical age: Journal of Geology, v. 105, p. 441–456.

Hsu, K. J., and Wissert, H. J., 1980, South Atlantic paleoceanography: Cambridge, UK, Cambridge University Press, p. 230–234.

Huber, B. T., Hodell, D., and Hamilton, C. P., 1995, Middle–Late Cretaceous climate of the southern high latitudes: Stable isotopic evidence for minimal equator-to-pole thermal gradient: Geological Society of America Bulletin, v. 107, p. 1164–1191.

Hudson, J. D., 1977. Stable isotopes and limestone lithification: Journal of the Geological Society of London, v. 133, p. 637–660.

Jacobsen, S. B., and Kaufman, A. J., 1999. The Sr, C, and O isotopic evolution of Neoproterozoic seawater: Chemical Geology, v., 161, p. 37–57.

Jones, C. E., Hugh, C. J., Coe, A. L., and Hesselbo, S. P., 1994, Strontium isotopic variations in Jurassic and Cretaceous seawater: Geochimica et Cosmochimica Acta, v. 58, p. 3061–3074.

Kaufman, A. J. and Knoll, A. H., 1995, Neoproterozoic variations in the C-isotopic composition of seawater: Stratigraphic and biogeochemical implications: Precambrian Research, v. 73, p. 27–49.

Kha, L. C., Sherman, A. G., Narbonne, G. M., Knoll, A. H., and Kaufman, A. J., 1999, $\delta^{13}C$ stratigraphy of the Proterozoic Bylot Supergroup, Baffin Island, Canada: Implications for regional lithostratigraphic correlations: Canadian Journal of Earth Science, v. 36, p. 313–332.

Lahsen, A., and Charrier, R., 1972, Late Cretaceous ammonites from the Seno Skyring–Strait of Magellan area, Magallanes Province, Chile: Journal of Paleontology, v. 46, p. 520–532.

Magaritz, M., 1989, ^{13}C minima follow extinction event: a clue to faunal radiation: Geology, v. 17, p. 337–340.

Marquillas, R. A., Del Papa, C. E., and Sabino, I. F., 1999, Environmental variations during the Cretaceous–Paleogene: Salta Group Basin, northwest Argentina [ext. abs.], *in* VII International Symposium on Mesozoic Terrestrial Ecosystem, Actas, Buenos Aires, p. 38–39.

Mozley, P. S., and Burns, S. J., 1992, Oxygen and carbon isotopic composition of marine carbonates concretions: An overview: Journal of Sedimentary Petrology, v. 63, p. 73–83.

Palma, R. M., 1984, Características sedimentológicas y estratigraficas de las Formaciones en el limite Cretácico Superior-Terciario Inferior, en la Cuenca Salteña. Universidad Nacional de Tucuman, Facultad de Ciencias Naturales, 239p.

Rollinson, H., 1994, Using geochemical data: evaluation, presentation, interpretation. Longman, 352 p.

Ruiz, C., 1965, Geología y yacimientos metalíferos de Chile: Santiago, Chile, Inst. Inv. Geolog., 305 p.

Salfity, J. A., and Marquillas, R. A., 1994, Tectonic and sedimentary evolution of the Cretaceous–Eocene Salta Group Basin, Argentina, *in* Salfity, J. A., ed., Cretaceous tectonics in the Andes: braunschweig-Wiesbaden, Germany, Friedrich Vieweg and Son, Earth Evolution Sciences, p. 266–315.

Salfity, J. A., Monaldi, C. R., Guidi, F., and Sales, R. J., 1998, Mapa geológico de la Província de Salta: Buenos Aires, Secretaría de Industria, Comercio y Minería, Servício Geológico Argetino, scale: 1:500,000.

Souza, R. S., Soldan, A. L., Henz, G., Takaki, T., Oliveira, J. B., Barrocas, S. B., Koutsoukos, A. M., and Botelho Neto, J., 1994, A passagem Cretaceo-Terciario na Peninsula Antartica: Proceedings of the 38th Congress of the Brasilian Geological Society, Camboriú, Santa Catarina, p. 357–358.